PostPrint

Spatio-temporal variation in sea state parameters along virtual ship route paths

Ulrik D. Nielsen[a,b]

[a] *DTU Mechanical Engineering, Technical University of Denmark,* Kgs. Lyngby, Denmark
[b] *Centre for Autonomous Marine Operations and Systems, NTNU AMOS,* Trondheim, Norway

Abstract

The article presents a study investigating the level of variation in sea state parameters encountered by sailing ships crossing the oceans. The sea state parameters have been obtained from a reanalysis, in this case the ERA5. The study is based on the use of different interpolation schemes to compute parameters in geographical positions off the fixed grid. It is shown that the variation in sea state parameters can be significant. Consequently, in case of sailing ships, covering relatively long distances in a short time (30-60 minutes), it is recommended to rely on bilinear interpolation rather than nearest neighbour. The variation in the sea state parameters is, in fact, at a level which means that the normal assumption of a stationary seaway in periods up to 3 hours likely is violated for ships sailing the typical service speed (15 – 20+ knots).

Keywords:
Sea state parameter variation, ERA5, spatial interpolation, ship operations

1. Introduction

1.1. Context

The effect of waves and wind on design and operation of marine structures is undisputable, and over time a vast number of studies have addressed the resulting importance to collect metocean data. In the more recent years, global reanalyses resulting in ocean wave databases have become readily accessible to both researches and commercial applications in, for instance, ship performance evaluations, addressing fuel efficiency and environmental aspects as well as safety issues. One example of a global reanalysis is produced by the Copernicus Climate Change Service funded by the EU [1]. This particular reanalysis is managed by the European Centre for Medium-range Weather Forecasts (ECMWF) and is made using their wave model ECWAM [2]. The outcome of the reanalysis is denoted by ERA5, as a short for 'ECMWF ReAnalysis' and

Email address: udn@mek.dtu.dk (Ulrik D. Nielsen)

referring to the fifth major reanalysis [3]. It is essential to mention that the ERA5 is produced by running atmospheric and ocean models in interaction, and obviously a relevant role is played by the wind forcing derived as the atmospheric component in the models' chain. That is, in order to have good wave data, good winds are mandatory. The point of this study is, however, not to discuss the absolute accuracy of the ERA5 database in a comparison with observations. As a result, the study contains no discussions about atmospheric conditions but focuses on the wave conditions alone.

1.2. Motivation and research questions

The output of a reanalysis is connected to a pre-defined space-time grid, where geographical coordinates describe the spatial variation of the output. In principle, the space-time grid can be refined to any resolution but at the cost of large computational efforts thus leading to constraints for practical reasons; for instance, the spatial distance can be 0.5-1.0 degrees (longitude and latitude) as often considered in normal practice. In ship performance evaluations, the given ship navigates on a route from point A to point B. As the route path only rarely is exactly on top of one of the fixed grid points, the wave conditions must for most part of the route be estimated by interpolating between adjacent points, where one alternative is to use the wave conditions at the nearest grid point as an approximation. Another condition of ship performance analyses is the fact that the considered voyages are often several days in length as entire oceans are crossed. In the specific analysis of a voyage, the (total) period in question is therefore segmented into a lot of 30-60 minutes time windows within which the seaway is assumed to be stationary. In other words, the sea state and the corresponding integral wave parameters are approximated as constant in the given time window. Note that in this study *integral wave parameters* and *sea state parameters* are used interchangeably.

Having had the context and motivation set forth, three relevant research questions to consider are listed below; all with attention to the situation of a mapped ship route curving through a large set of points on a fixed grid. Furthermore, it should be kept in mind that cargo ships, like container ships, often sail with speeds of more than 20 knots, thus travelling relatively long distances during aforementioned 30-60 minutes time windows. The present study builds on the following questions: (1) Generally, what level of spatio-temporal variation can be expected in sea state parameters when the proximate grid points are considered? (2) What interpolation scheme is reasonable considering an arbitrary position; nearest neighbour, bilinear, or bicubic interpolation? (3) To what extent is the seaway (truly) stationary?

It must be emphasised that the questions essentially have their mere relevance in a context where the wave conditions, as modelled by the energy balance equation (see subsection 2.1), are computed in a discrete

set of fixed points at discrete time-steps. The questions are therefore resulting due to practical constraints in connection with spectral wave modelling that requires high computational power.

1.3. Scope and restrictions

This study investigates the spatio-temporal variation in sea state parameters obtained with the ERA5 data. In an application-oriented view, the study has relevance to problems concerned with ship performance analyses, where interpolation to geographical points off the grid is necessary. Hence, the study considers the implication of using different interpolation schemes aimed at the ERA5 data. As indicated, attention is focused on wave conditions in terms of sea state parameters such as significant wave height, zero-crossing period, and mean wave direction. On the other hand, it is well-known that the performance of ships, in general, is affected by not only the waves, but of course also by winds and currents. In this sense, the study considers only a subset of the metocean data that could be relevant to consider in a complete study. Furthermore, and maybe more importantly, the study restricts itself to study the variation in wave conditions solely; that is, the resulting consequence for subsequent analyses of ship performance with respect to, say, wave-induced motions and added resistance in waves [4, 5] is not addressed. In an application context regarding ship performance, the present work is therefore just considered as a first step towards a much more extensive and complete study. Finally, it is noteworthy that the study is limited to consider results of only the ERA5 wave database, resulting from the ECWAM, while estimates from similar models, e.g. WAVEWATCH III [6, 7], are not included.

1.4. Related literature

Numerous publications address the importance to collect weather and wave data for purposes connected to marine design and operation, not to mention the huge special literature about means (e.g., buoys, remote sensing, wave radar) for actual observations and numerical prediction models such as third generation spectral wave models, possibly including data assimilation. In this paper, there is no intention to review the large literature, but a few publications can benefit reading, in addition to the references already mentioned in the preceding. A general overview and review related to in-situ observations of sea states has been given by [8] and another reference on ocean wave measurements techniques is [9], noting that in-situ observations can be supplemented with estimates along the route of a ship using the wave buoy analogy [10, 11], where the ship itself acts as a wave sensor. General references on ocean waves physics, measurements and modelling are, for instance, [12–14]. Validation of predictions of metocean data has been conducted by, e.g.,

[15–17], while dedicated applications of the ERA5 data together with the use of wave forecasting for wave-ship response assessment through weather routing can be found in for instance [18–25]. The current study has some resemblance to the work presented in [26] that looks at the impact of weather source selection on time-and-place specific vessel response predictions. However, the aforementioned study [26] does not consider the impact (i.e. variation) related to positional interpolation along the route path of a vessel, and as presented above this is the objective of the present paper. Another important study to mention within the set scope is [27] that discusses the effect of intrinsic and sampling variability on wave parameters and wave statistics. Thus, it is concluded "that the length of a wave record is critical for evaluating stable parameters as far as possible in varying sea states". As will be seen later, the present study support this point but it also becomes evident that the statistics of wave conditions generally vary quite a lot in space and time.

1.5. Composition

After the introduction, Section 2 outlines the fundamentals and the methodology of the study, including the basics of spectral wave modelling together with remarks about the calculation of (interpolated) sea state parameters. Section 3 presents the results of the work, specifically the section considers and discusses the variation and uncertainty in sea state parameters as observed from sailing ships operating on realistic shipping routes. Finally, concluding remarks are given in Section 4.

2. Fundamentals and methodology

2.1. Basics of reanalyses and ERA5

Essentially, atmospheric reanalyses provide estimations of coherent records of global air-sea-land circulation [28, 29]. Focusing on sea surface conditions, the spatio-temporal development of ocean wave systems can be described by the energy balance equation [6, 30–32]. Specifically, using third generation spectral wave models, the time- and position-dependent wave spectrum is computed by integration of the energy balance equation, without any prior restriction on the spectrum shape. In addition, observations of wind and waves are assimilated.

The ERA5 hourly ocean wave data on single levels [33], as used in this study, is available on a regular latitude-longitude grid at $0.5^\circ \times 0.5^\circ$ resolution with updates every 60 minutes. A complete list of available ocean and sea state parameters can be found in [2]. In the present study, only three of the standard parameters used within naval architecture are considered, and their definitions follow in subsection 2.3.

The ERA5 dataset includes 4D-Var assimilation [34], which takes account of the exact timing of the observations and model evolution within the assimilation window. The assimilation system is able to estimate biases between observations and to sift good-quality data from poor data. At the same time, the laws of physics allow for estimates at locations where data coverage is low.

2.2. Motivation of study revisited

With due account to the basics of reanalyses, a more scientifically sound motivation of the study can now be formulated: In realistic conditions, analytical solutions for the wave energy balance equation do not exist. Hence, it is necessary to adopt numerical approaches that mandatorily require discretisation on a space-time grid, or as an alternative, spectral grids based on sets of orthogonal functions, e.g. Fourier series. In this framework, in order to attain a high level of detail, a very fine space-time grid is needed. Consequently, computational constraints come in by imposing limits on the maximum number of space-time grid points, i.e. on the attainable level of space-time resolution. Finally, when archiving and/or disseminating the output data from forecast models, data archiving and data transmission constraints may further limit the resolution, by imposing data decimation protocols. Typically, while the computational time-step of wave models is of the order of minutes, the output is on an hourly (or three, or six hourly) basis. As a consequence of all of this, the final user of wave model output data needs to adopt some sort of interpolation in space and/or in time, if the available model resolution is not sufficient for the particular application.

2.3. Integral wave parameters

The statistics of ocean wave systems can be derived from the directional wave spectra characterising the particular wave systems. It is not practical, however, to compare wave spectra, one by one. Consequently, it is decided to compare integral wave parameters, also referred to by sea state parameters. In the comparisons made later, the following parameters are considered: significant wave height H_s, zero-upcrossing period T_z, and mean wave direction D_m; all derived from the directional wave spectrum $E(\omega, \mu)$,

$$H_s = 4\sqrt{m_0} \tag{1}$$

$$T_z = 2\pi\sqrt{\frac{m_0}{m_2}} \tag{2}$$

$$D_m = \text{atan}(d/c) \tag{3}$$

$$\tag{4}$$

where

$$m_n = \int_0^{\infty} \omega^n F(\omega)\, d\omega \quad n = \{0, 2\} \tag{5}$$

$$F(\omega) = \int_{-\pi}^{\pi} E(\omega, \mu)\, d\mu \tag{6}$$

$$d = \int_{-\pi}^{\pi} \int_0^{\infty} E(\omega, \mu) \sin(\mu) d\omega d\mu \tag{7}$$

$$c = \int_{-\pi}^{\pi} \int_0^{\infty} E(\omega, \mu) \cos(\mu) d\omega d\mu \tag{8}$$

with ω as the circular frequency in [rad/s] along the wave direction μ.

2.4. Interpolation schemes

As explained by [36], the ERA5 data is produced and archived on a reduced Gaussian grid which is a series of evenly spaced data points on each 'spherical circle' (latitude), and parallels (longitude) spaced at quasi-regular intervals, cf. Figure 1. All gridded data is made available in decimal degrees, with latitude values in the range [-90;+90] referenced to the equator and longitude values in the range [0;360) referenced to the Greenwich Prime Meridian.

Figure 2 illustrates a situation when a ship, en-route, is in the proximity of four neighboring grid points. The situation reflects an exact point in time at which the ERA5 data is available; that is, the instant coincides with the hourly update produced by the ERA5. In this case, the sea state parameters, at the position of the ship, can be obtained by interpolation, where 'nearest neighbour' and bilinear interpolation are the two simplest interpolation schemes. Alternatively, bicubic interpolation can be made but, in contrast to bilinear interpolation which considers 4 points in total, cubic interpolation requires four grid points in each dimension giving a total of 16 points.

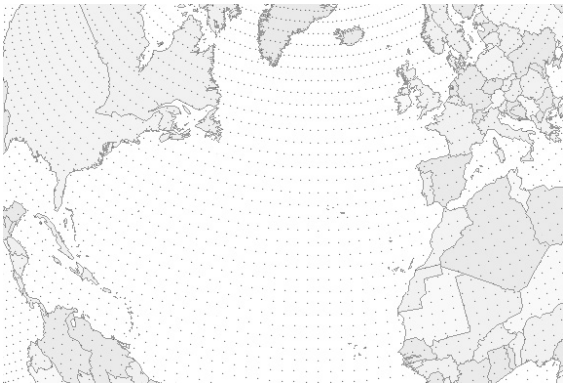

Figure 1: Illustration of (part of) the Gaussian grid used for ERA5. [35]

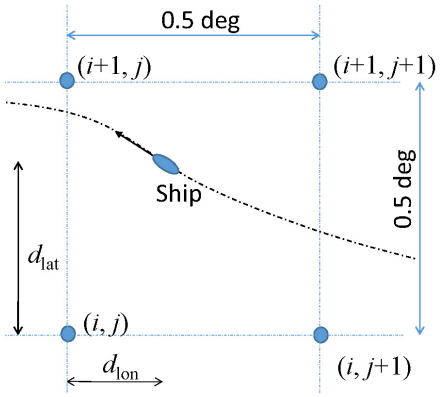

Figure 2: The instant when a ship en-route is in the vicinity of four neighboring grid points. The single grid point is indexed by the pair (i, j), where i refers to latitude and j refers to longitude. The distance between point (i, j) and the ship is given by the Euclidian distance using d_{lat} and d_{lon}, neglecting the Earth's curvature due to the short distance between consecutive waypoints.

Interpolation in significant wave height H_s and in zero-upcrossing period T_z is straightforward. In contrast, mean wave direction is circular, leading to the ambiguity that $D_m = 0$ deg and $D_m = 360$ deg are equivalent. As a result, bilinear or bicubic interpolation in mean wave direction, based on values from more than one grid point, may be distorted, and so can a comparison between a corresponding pair of interpolants, e.g., nearest neighbour vs. bilinear. The interpolation in wave direction is therefore based on the Cartesian vector components of the particular directions that enter the interpolation. To account for any variation in significant wave height from grid point to grid point, the interpolation is weighted by H_s. Consequently, interpolation in (mean) wave direction is based on a new set of parameters (A, B) calculated for all grid points (i, j), with:

$$A(i,j) = H_s(i,j) \cdot \cos(D_m(i,j)) \tag{9}$$

$$B(i,j) = H_s(i,j) \cdot \sin(D_m(i,j)) \tag{10}$$

In this case, interpolation at an arbitrary point off the grid can be made in both A and B using the required interpolation scheme, for instance, bilinear interpolation, cf. Figure 2. The mean wave direction at the considered geographical point, corresponding to any given time and position represented by index k is subsequently calculated as,

$$D_{m,k} = \text{atan2}(B_k, A_k) \tag{11}$$

where B_k, A_k are the interpolated Cartesian vector components based on Eq. (9) at the considered time-

position instants $k = 1, 2, ..., K$.

As introduced, directional ambiguity also implies that a comparison between a corresponding pair of wave directions is slightly delicate, and this is discussed below in subsection 2.5.

Section 3 presents the results of the work, where focus is on the spatio-temporal variation in sea state parameters as encountered along virtual shipping routes. It should be noted, however, that it is in fact merely the influence of *spatial interpolation* which is investigated. That is, the study does investigate how sea state parameters vary with time, but it does not attempt to make a sophisticated temporal interpolation, other than using nearest neighbour. This is more clearly explained in section 3.

2.5. Statistics of absolute values and deviations

The spatio-temporal variation of sea state parameters and the influence of a specific interpolation method will be based on a set of statistical metrics using both absolute measures and (relative) deviations. The calculation of absolute statistics, such as mean value and standard deviation, is straightforward for H_s and T_z. Similarly, the statistics of deviations between a corresponding pair of estimates are easily calculated from the following measures, showing the relative deviations of H_s and T_z

$$\varepsilon_{k,Hs}(\alpha \text{ vs. } \beta) = \frac{|H_{s,k}^{(\alpha)} - H_{s,k}^{(\beta)}|}{H_{s,k}^{(\beta)}} \tag{12}$$

$$\varepsilon_{k,Tz}(\alpha \text{ vs. } \beta) = \frac{|T_{z,k}^{(\alpha)} - T_{z,k}^{(\beta)}|}{T_{z,k}^{(\beta)}} \tag{13}$$

noting that $|\cdot|$ is the L2 norm, and index k refers to any one specific point in time, and thus space, with a corresponding pair of estimates (α, β) from two different interpolation schemes α and β, for instance "α = nearest neighbour" and "β = bilinear interpolation".

The circularity of wave direction implies that the mean value $D_{m,\text{mean}}$ of a sequence of mean wave directions at arbitrary geographic points must be based on the Cartesian vector components of the mean wave direction in the particular geographical points; equivalent to how interpolation in wave direction was made, cf. Eqs. (9) and (11), but without the H_s-based weighting. In quantitative terms, the formula becomes,

$$D_{m,\text{mean}} = \text{atan2}(\bar{B}, \bar{A}), \tag{14}$$

$$\bar{A} = \frac{1}{K}\sum_{k=1}^{K} A_k, \; \bar{B} = \frac{1}{K}\sum_{k=1}^{K} B_k \tag{15}$$

The corresponding standard deviation σ is calculated in line with the mathematical definition of standard deviation. Specifically, it is obtained by

$$\sigma^2 = \frac{1}{K}\sum_{k=1}^{K}(\min_{abs}\{D_{m,k} - D_{m,\text{mean}}\})^2. \tag{16}$$

where the minimization function $\min_{abs}\{\cdot\}$ is applied to ensure that it is always the minimum difference, in absolute terms, which is computed, i.e. $(D_{m,k} - D_{m,\text{mean}}) < 180$ deg always, thus addressing that wave direction is circular.

The statistics of the deviation between a corresponding pair of estimates of mean wave directions are obtained from the following measure

$$\varepsilon_{k,Dm}(\alpha \text{ vs. } \beta) = |\min_{abs}\{D_{m,k}^{(\alpha)} - D_{m,k}^{(\beta)}\}| \tag{17}$$

emphasising that the deviation, in this case, is kept in dimensional form, as wave direction is circular, and, again, that the minimization function $\min_{abs}\{\cdot\}$ ensures that the deviation between the pair of estimates is less than 180 deg.

3. Results and discussions

In the following, the attention is on the spatial variation of sea state parameters, in terms of H_s, T_z, and D_m, cf. Eqs. (1), (2), and (3), as experienced from sailing ships. The considered wave data along the virtual shipping routes is obtained from the ERA5 dataset [33].

3.1. Virtual shipping routes

The study builds on the situation of ships sailing on particular routes crossing the larger oceans. The studied data has its background in real voyages, as four realistic ship routes are simulated. The considered routes are illustrated in Figure 3, and it is noted that all routes are specified as great circle paths for simplicity; thus, the land-points at Newfoundland, passed on the route Le Havre to Halifax, are simply discarded. In realistic situations, cargo ships normally sail at speeds from 10 to more than 20 knots on ocean crossings, obviously depending on ship type and environmental conditions. In this study, the ship speed is fixed to a constant value, but neglecting the influence of weather and waves on operations, and each ship route has been simulated with speeds 15, 20, and 25 knots.

As indicated earlier, wave-induce response analyses and fuel performance evaluations of ships often assume that the sea state remains stationary in periods of about half an hour up to a few hours. Hence, it is

decided to estimate the sea state parameters along the particular vessel routes with 30 minutes updates. In principle, such an updating frequency requires a (delicate) *temporal* interpolation, in addition to the spatial interpolation, since the ERA5 data comes with estimates only every 60 minutes. In this study, the temporal interpolation is based on nearest neighbour. This means that every second site-specific update coincides with the regular ERA5 temporal update, say, at time t_k, while the site-specific update in between the regular ERA5 updates is based on the (same) time t_k, but taking into account the change in ship position due to the distance covered in 30 minutes. In the remaining part of the paper, it is always given that the temporal interpolation is based on nearest neighbour.

In order to achieve statistically reliable results, it is decided to simulate a number of voyages on each route, cf. Figure 3. Thus, letting a ship depart on each and every day over a whole year, a total of 366 (=365+1) voyages are simulated on each route at each speed, selected as 15, 20, or 25 knots. Specifically,

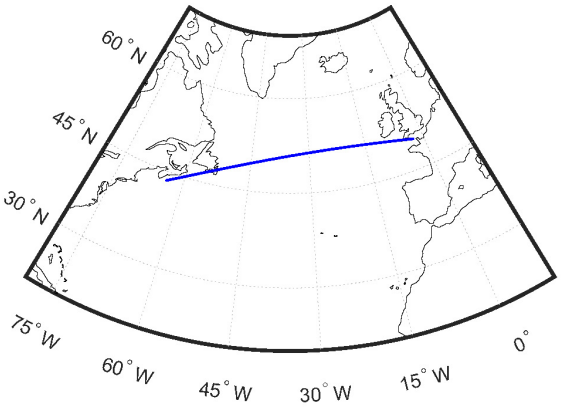

(a) Le Havre to Halifax, distance = 4,585 km.

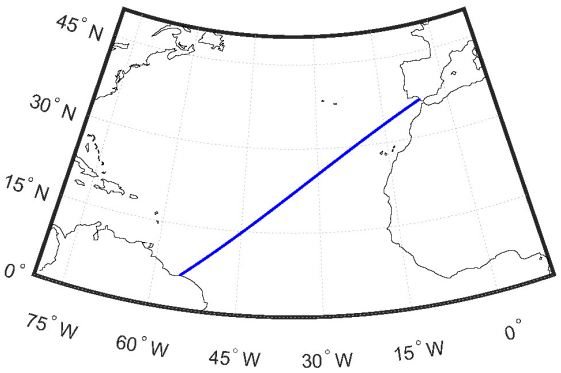

(b) Cadiz to Paramaribo, distance = 6,000 km.

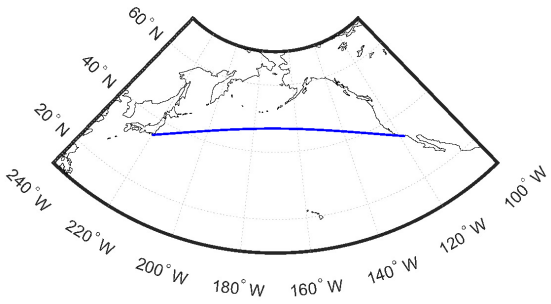

(c) Yokohama to Los Angeles, distance = 8,825 km.

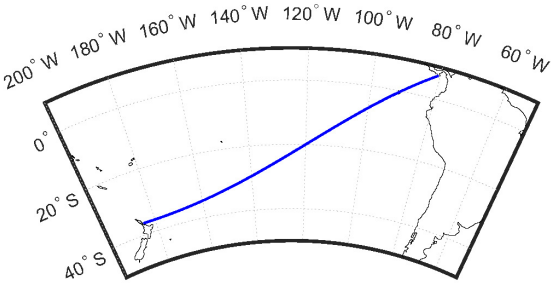

(d) Panama City to Auckland, distance = 11,700 km.

Figure 3: The great circle paths of the virtual shipping routes.

the year 2016 is chosen with the first voyage departing on 01 January and with the last on 31 December; noting that the particular year is selected for no special reasons.

3.2. Comparison of interpolation schemes

As illustrated in Figure 2 it is necessary to interpolate among the available grid points to obtain the sea state parameters at the actual position of the vessel; simply because the ship with very little chance is exactly on top of a grid point, exactly at the time when the ERA5 update is available. The two simplest interpolation schemes are nearest neighbour and bilinear interpolation. It should be realised that, for a grid spacing of 0.5 deg, the maximum distance between a ship and one of the ERA5-grid points is less than 28 km at any point in time. This is at the equator, while the distance reduces the farther north, or south, of it. Hence, with little need to say, if the sea state were to change only slowly and over substantial distance (+100 km), there were to be an almost perfect agreement between the integral wave parameters obtained by the two interpolation schemes. For the specific voyages, the comparison of the results can be seen in Figures 4-6, presenting the outcome for significant wave height, zero-crossing period, and mean wave direction, respectively, and with all figures applicable for a speed of 20 knots. Specifically, any plot from Figures 4-6 shows the direct comparison between corresponding pairs of interpolants, i.e. nearest neighbour vs. bilinear. Based on the comparisons, some immediate observations and remarks are noteworthy: (1) Generally, the scattering around the line of identity, considering all three parameters, is merely an indication of the effect to be positioned in a point off the fixed grid; that is, the scattering is simply a measure of the spatial variation in the sea state parameter(s). (2) The ambiguity in wave direction occurring at 0 deg and 360 deg is what makes the plots for D_m slightly dispersed around the line of identity at the zones in the vicinity of 0 deg and 360 deg; realising that, apparently, in a few cases the wave direction at the nearest grid point of the ship is closer to 360 deg from below ($D_m < 360$ deg), while interpolation among the proximate four grid points yields a wave direction closer to 0 deg from above ($D_m > 0$ deg), and/or vice versa. Obviously, in the specific cases, the calculation of the associated deviation between the corresponding pair of estimates must account for this circular behaviour of direction, cf. Eq. (17). (3) There appears to be no trends or tendencies in the comparisons, and generally the agreement, equivalently correlation, between the interpolants is assessed to be in line with expectation.

The plots in Figures 4-6 contain, as additional text-legends, the quantification of the agreement between the interpolation methods. Thus, the plots present the coefficient of determination R^2 (or "R-squared"), the root mean squared error (RMSE), and the 95-percentile, where the latter is the number 'p95' indicating

that 95% of corresponding pairs have a deviation less than the value p95. Extracts of the detailed statistics are also presented in Table 1, noting that the table presents both absolute statistics and statistics of the deviations. The absolute statistics show the mean ('Mean'), the standard deviation ('StD') and the maximum value ('Max') of the studied sea state parameters (H_s, T_z, D_m), as observed during all voyages made in the particular year. As expected, it can be seen that the absolute "yearly-based average" statistics essentially do not depend on the interpolation method, including bicubic interpolation. Besides, it is noted that the routes Le Havre to Halifax, crossing the North Atlantic, and Yokohama to Los Angeles, crossing the Northern Pacific, have the most severe wave conditions with an almost identical significant wave height.

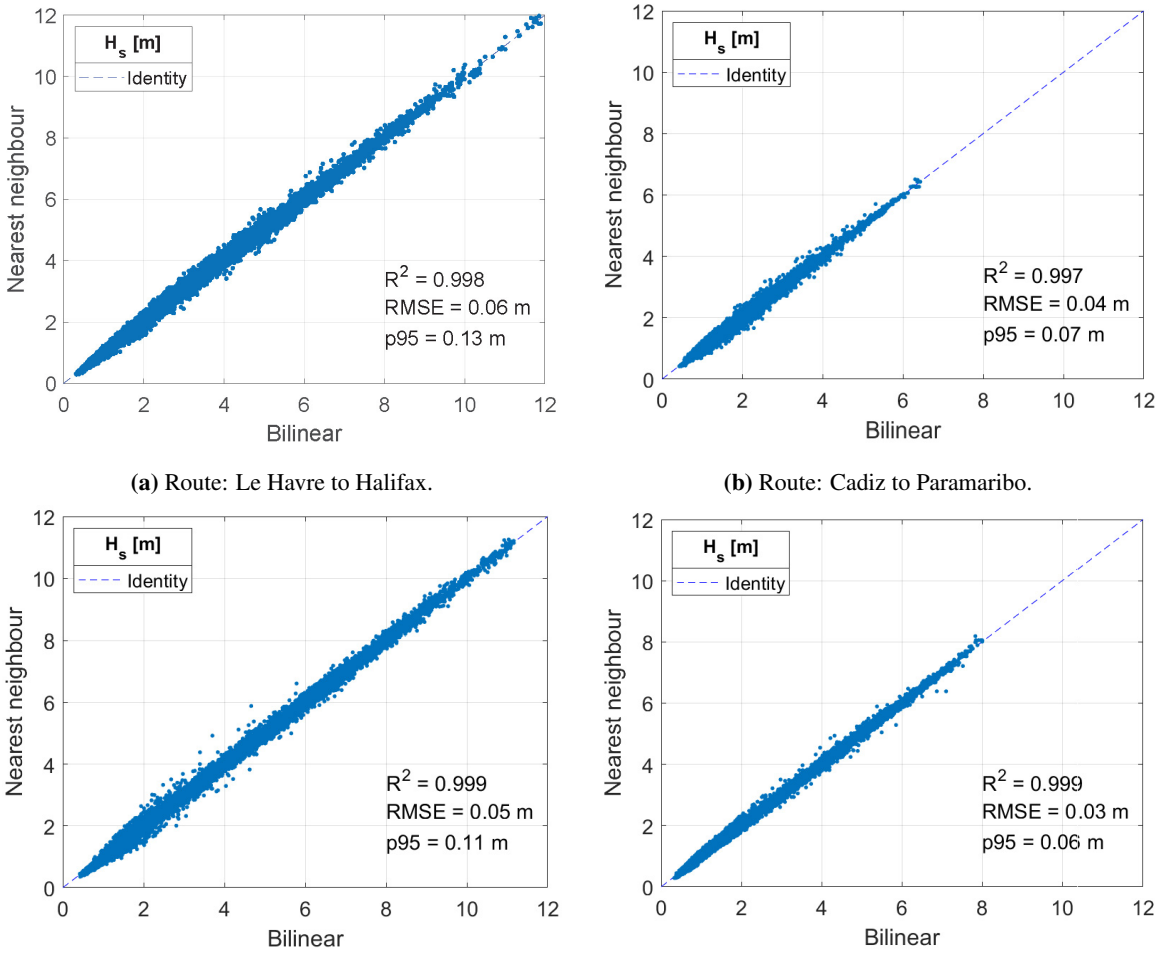

(a) Route: Le Havre to Halifax.

(b) Route: Cadiz to Paramaribo.

(c) Route: Yokohama to Los Angeles.

(d) Route: Panama City to Auckland.

Figure 4: Comparison between results for **significant wave height** obtained using nearest neighbour and bilinear interpolation. Ship speed is 20 knots. Note: R^2 is the coefficient of determination, RMSE is the root mean square error, p95 is the 95-percentile, where the "error" measure is based on Eq. (12).

The statistics of the deviations can be used to investigate the spatial variation of the sea state parameters, and to assess the effect of the selected interpolation method. As noted, Table 1 contains two sets of comparative results: 'Nearest neighbour vs Bilinear interpolation' and 'Bilinear vs. bicubic interpolation', comparing the effect of the chosen interpolation method. The comparison between nearest neighbour and bilinear interpolation is a direct measure of the spatial variation of the studied sea state parameter. For the significant wave height, it is observed that the (relative) variation can be up to as high as about 35-55%, but in the majority of cases the variation is less than approximately 5%. Specifically, to take the route Le Havre to Halifax as an example, the average variation with respect to H_s is 3.6%, taken as the RMSE value, and

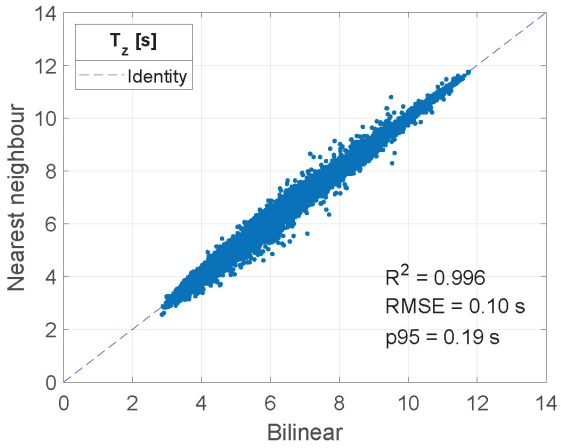

(a) Route: Le Havre to Halifax.

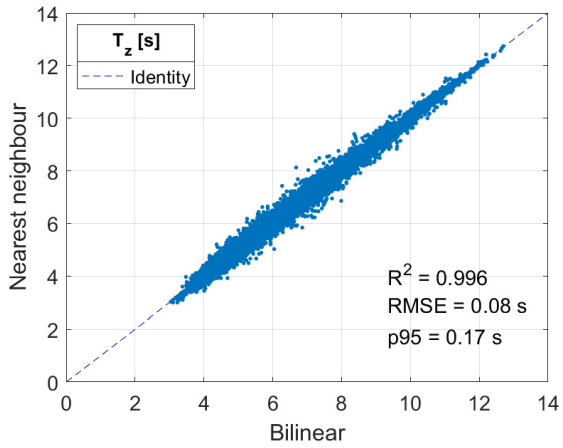

(b) Route: Cadiz to Paramaribo.

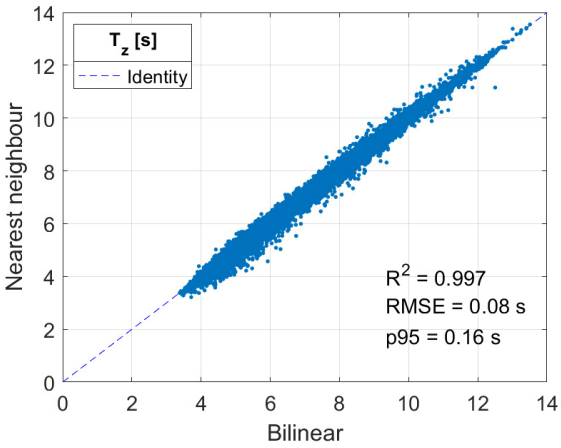

(c) Route: Yokohama to Los Angeles.

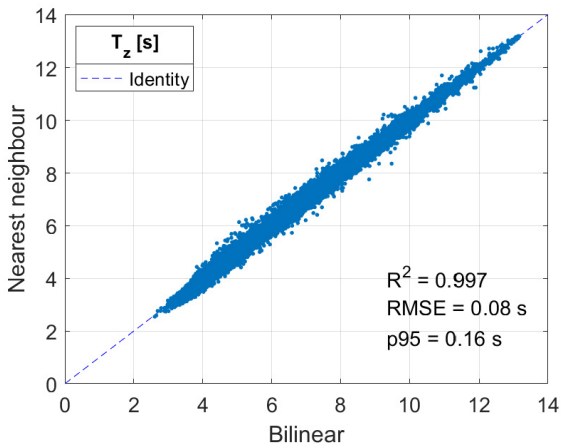

(d) Route: Panama City to Auckland.

Figure 5: Comparison between results for **zero-crossing period** obtained using nearest neighbour and bilinear interpolation. Ship speed is 20 knots. Note: R^2 is the coefficient of determination, RMSE is the root mean square error, p95 is the 95-percentile, where the "error" measure is based on Eq. (13).

the 95-percentile is 4.8%, which means that the (relative) variation is less than 4.8% in 95% of the cases. The listed maximum relative deviation for significant wave height corresponds to the dimensional values 0.76 m (37%), 0.62 m (44%), 1.2 m (52%), and 0.72 m (35%) for the four routes LH, CP, YL, and, PA, respectively, when interpolation by nearest neighbour is compared against bilinear interpolation. In more general terms, including zero-crossing period and mean wave direction, it is evident that the spatial variation in sea state parameters can be significant. In an application-oriented context, having a focus on, say, ship performance analyses with respect to wave-induced motions and ship resistance, this finding indicates that it can be influential to select the sea state parameters by bilinear interpolation, i.e. at the actual point

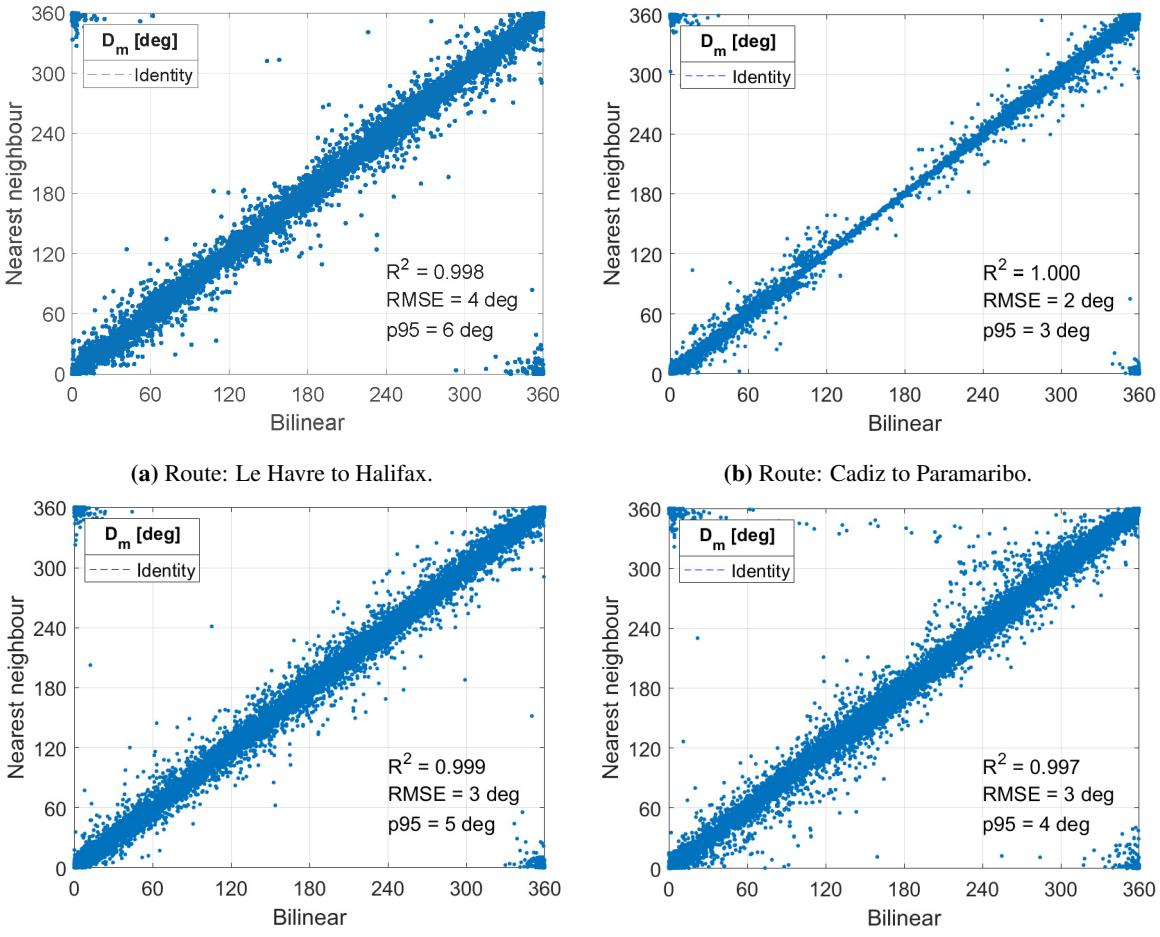

(a) Route: Le Havre to Halifax.

(b) Route: Cadiz to Paramaribo.

(c) Route: Yokohama to Los Angeles.

(d) Route: Panama City to Auckland.

Figure 6: Comparison between results for **mean wave direction** obtained using nearest neighbour and bilinear interpolation. Ship speed is 20 knots. Note: R^2 is the coefficient of determination, RMSE is the root mean square error, p95 is the 95-percentile, where the "error" measure is based on Eq. (17).

Table 1: Statistics of the sea state parameters depending on the interpolation methods. LH: Le Havre to Halifax. CP: Cadiz to Paramaribo. YL: Yokohama to Los Angeles. PA: Panama City to Auckland. Ship speed is $U = 20$ knots. The statistics of the parameters and of the deviations are based on the formulas in subsection 2.5.

	H_s [m]				T_z [s]				D_m [deg]			
	LH	CP	YL	PA	LH	CP	YL	PA	LH	CP	YL	PA
Absolute statistics												
Nearest neighbour:												
Mean	2.93	2.06	2.93	2.35	6.38	5.98	6.50	6.69	268	27	269	193
StD	1.48	0.64	1.52	0.81	1.44	1.23	1.45	1.35	72	48	70	60
Max	12.3	6.51	11.3	8.19	11.7	12.7	13.5	13.2	N/A	N/A	N/A	N/A
Bilinear interpolation (actual point):												
Mean	2.93	2.06	2.95	2.37	6.37	5.98	6.51	6.69	268	28	269	193
StD	1.48	0.63	1.52	0.80	1.43	1.22	1.45	1.34	72	47	70	60
Max	12.2	6.43	11.2	8.01	11.8	12.7	13.5	13.2	N/A	N/A	N/A	N/A
Bicubic interpolation (actual point):												
Mean	2.99	2.08	3.01	2.39	6.44	6.02	6.52	6.71	269	28	268	193
StD	1.48	0.62	1.53	0.79	1.42	1.22	1.44	1.33	70	45	68	59
Max	12.2	6.44	11.2	8.02	11.8	12.8	13.4	13.2	N/A	N/A	N/A	N/A
Statistics of deviations												
Nearest neighb. vs. Bilinear interpolation:												
R^2	0.998	0.997	0.999	0.999	0.996	0.996	0.997	0.997	0.998	1.000	0.999	0.997
RMSE	0.06	0.04	0.05	0.03	0.10	0.08	0.08	0.08	4	2	3	3
RMSE*	3.6%	2.7%	3.2%	2.0%	4.0%	3.3%	3.1%	3.0%	N/A	N/A	N/A	N/A
Max	0.76	0.62	1.22	0.72	1.49	1.45	1.35	1.12	163	86	170	178
Max*	37%	44%	52%	35%	26%	20%	30%	18%	N/A	N/A	N/A	N/A
p95	0.13	0.07	0.11	0.06	0.19	0.17	0.16	0.16	6	3	5	4
p95*	4.8%	3.5%	3.6%	2.4%	3.2%	2.8%	2.5%	2.4%	N/A	N/A	N/A	N/A
Bilinear vs. bicubic interpolation:												
R^2	1.000	1.000	1.000	1.000	1.000	1.000	1.000	1.000	1.000	1.000	1.000	1.000
RMSE	0.01	0.01	0.01	0.00	0.02	0.02	0.01	0.02	0	0	0	1
RMSE*	1.0%	1.0%	0.0%	0.0%	0.0%	0.0%	0.0%	0.0%	N/A	N/A	N/A	N/A
Max	0.26	0.14	0.22	0.13	0.32	0.25	0.13	0.35	45	20	32	53
Max*	6.0%	4.4%	5.5%	9.0%	4.8%	3.9%	2.5%	8.0%	N/A	N/A	N/A	N/A
p95	0.02	0.01	0.01	0.01	0.03	0.03	0.03	0.03	1	0	1	1
p95*	1.0%	1.0%	0.0%	0.0%	0.0%	0.0%	0.0%	0.0%	N/A	N/A	N/A	N/A

*Relative deviation; applicable to H_s and T_z only.

of operation, in contrast to selecting the parameters at the nearest available grid point. On the other hand, the results in Table 1 indicate that it makes little difference to interpolate using bilinear and bicubic interpolation, as the obtained estimates are essentially the same. Thus, it is seen that both the RMSE and the p95 values are insignificant for all integral wave parameters (H_s, T_z, D_m); it is just on the maximum values that notable variations can be found. However, it is important to emphasise that confirmative conclusions in these directions cannot be made before a specific study has been conducted. This will require a sensitivity

analysis of ship performance indicators with regards to the evaluated distribution of the discrepancies between the results of the different interpolation approaches. Moreover, it would be interesting to search for a numerical quantification of the threshold discrepancies in metocean parameters variability beyond which ship performance indicator variations are not negligible. These limits could be dependent on each different ship and specific performance indicator, and on the ship service operational environment under study. Only after such analyses, based on careful and comprehensive numerical evaluations, there will be justified evidence with respect to the importance of interpolation schemes. As a final comment to the statistics shown in Table 1, it is interesting to note that, although the physical distance in kilometres between grid points is the smallest for the route Le Havre to Halifax, this route still has the largest (average) variation in the sea state parameters, when measuring from the actual point to the nearest grid point. This observation is not unexpected and can be considered as a kind of evidence that the North Atlantic generally is one of the harshest oceans to sail in, and conditions can quickly change.

As mentioned previously, the four virtual routes were also simulated at two other speeds, i.e. $U = 15$ knots and $U = 25$ knots, but results are not shown as the statistics of the absolute parameters and of the deviations are very similar, compared to the results for $U = 20$ knots. This is so for the comparison of interpolation methods, but for the short-term variation of the sea state parameters at consecutive waypoints, a dedicated study is necessary, and this is presented in the next subsection.

3.3. Variation in sea state parameters at consecutive waypoints

The previous subsection studied the variation in sea state parameters observed because of different spatial positions. In this sense, for frozen time, the consequence of being at two different but fairly close positions was considered. As a slight modification, the current part of the study investigates what level of variation in sea state that occurs as a result of evolvement in both space and time. That is, the idea is to compare the sea state parameters observed from a ship at a waypoint at time t_k with the parameters observed at a waypoint at a later time $t_k + \Delta t$, emphasising that in this case any variation results because of the evolvement Δt in time, and because the ship moves a distance $\Delta s = U \cdot \Delta t$ dependent on the ship's speed U. In the study, two situations are considered: 1) Consecutive waypoints are spaced by the sailing distance during $\Delta t = 1$h (= 60 minutes), 2) Consecutive waypoints are spaced by the sailing distance during $\Delta t = 3$h. Thus, in the given situation, the statistical metrics established in subsection 2.5 can be used to compare the sea state parameters at consecutive waypoints. However, for this sub-study, bilinear interpolation is used throughout, i.e. "$\alpha \equiv \beta$" in Eqs. (12)-(17), since it has just been found that this

interpolation scheme can be used with a reasonable accuracy for arbitrary points off the grid. The formulas of the (relative) difference[1] therefore reads, intentionally using Diff( ) to use another symbol than used with Eqs. (12)-(17),

$$\text{Diff}(H_{s,k}) = \frac{|H_{s,k} - H_{s,k+m}|}{H_{s,k}} \tag{18}$$

$$\text{Diff}(T_{z,k}) = \frac{|T_{z,k} - T_{z,k+m}|}{T_{z,k}} \tag{19}$$

$$\text{Diff}(D_{m,k}) = |\min_{abs}\{D_{m,k} - D_{m,k+m}\}| \tag{20}$$

where index $k+m$ represent a waypoint at a time later than the waypoint represented by index k; the value of m is set in accordance with $\Delta t = 1$h or $\Delta t = 3$h.

To have an overview of the general level of variation that can be expected when navigating the four routes, it is useful to study Figure 7. The figure shows the encountered distributions of sea state parameters on the four routes; with the parameters (H_s, T_z, D_m) on a given route oriented horizontally (row-wise). Specifically, the single plots show the probability density functions (PDF) of the parameters, obtaining the PDF by considering the data collected from all voyages on the given routes in the studied year (2016), keeping in mind that a new voyage is started on each and every day of the year. The empirical distributions of H_s and T_z are shown together with some of the standard PDFs, and it is observed that the Gumbel distribution is the best fit, in agreement with what can be anticipated from ocean wave statistics of annual extreme values, e.g. [37, 38]. Moreover, it is confirmed, as also reported in connection with the absolute statistics presented in Table 1, that the North Atlantic (Le Havre to Halifax) is the harshest of the ocean areas considered, although the PDFs of the Northern Pacific are quite similar.[2] In particular, it can be seen that these routes are dominated by waves coming from a westerly direction (270 deg). As the main observation from the set of PDFs, taking note also of the distances of the routes, generally the largest and most rapid variation in sea state parameters is anticipated on the route Le Havre to Halifax. Hence, it is decided to focus primarily on the route Le Havre to Halifax in the following.

Table 2 presents the overall statistical results of the analysis, while the detailed statistics can be observed from Figures 8 and 9 showing the PDFs of the computed differences, cf. Eqs. (18)-(20). It is noted that results are shown for the three different vessel speeds (15, 20, and 25 knots). The statistical parameters in Table 2 are in their definitions the same as those studied in the previous sub-study, cf. Table 1, albeit the

[1] Note that *difference* is used, as this term is considered more appropriate than *deviation* used in the previous sub-study.

[2] Strictly speaking, the finding applies to the particular routes in study; and *not* to the ocean(s) as a whole.

coefficient of determination is left out. Based on the numbers in Table 2 it is seen that substantial variation in the sea state parameters can occur. The main observations are the following: (1) The statistics (RMSE, Max, p95) and thus variation depend on ship speed, naturally encountering more variation as the speed increases; (2) Similarly, the variation increases significantly when the distance between waypoints is based on updates

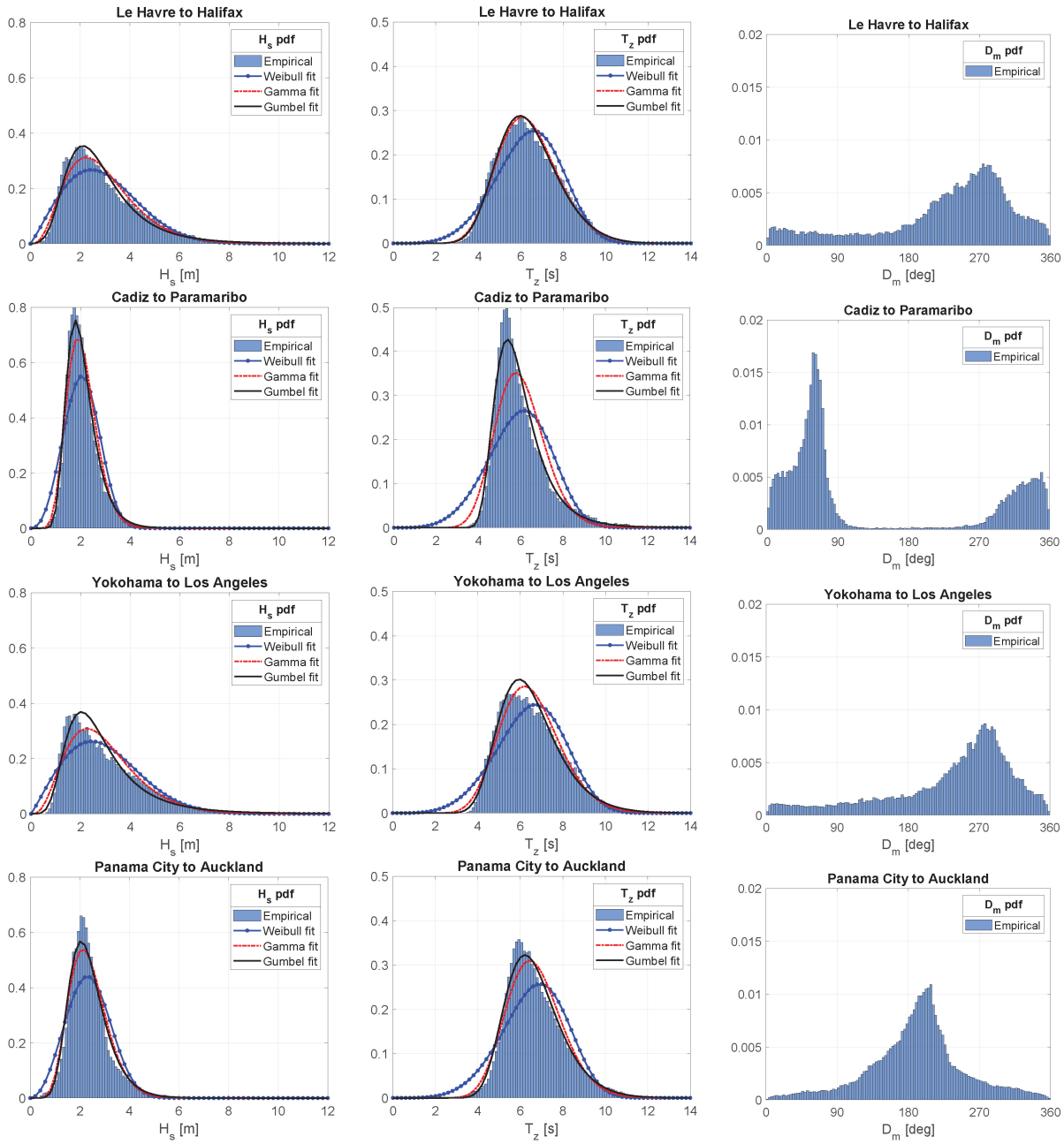

Figure 7: Probability density functions of encountered sea state parameters along the four studied routes.

every 3h compared to 1h updates; (3) The variation in significant wave height is more pronounced than for zero-upcrossing period, but it is evident that all sea state parameters, including mean wave direction, tend to vary a lot in just one hour of sailing. Especially, the maximum difference in a parameter, as obtained at two consecutive waypoints, can be large, but also the majority of cases, as represented by the 95-percentile, will show relatively large differences. For instance, it is seen that for 5% of the cases, the differences at two consecutive waypoints, spaced by a distance equivalent to 1h of sailing, are larger than 9.7%, 7.0%, and 17 deg in, respectively, H_s, T_z, and D_m; even at the lowest speed (15 knots).

Graphical illustrations of the statistics are given by the PDFs shown in Figures 8 and 9 applicable to $\Delta = 1$h and $\Delta = 3$h, respectively. It can be seen that the empirical PDFs are fitted with two parametric PDFs; the normal and the t location-scale distributions, where the latter is also sometimes known as the Skewed Student t-distribution [39, 40]. By nature, the normal distribution could be expected to be a good

Table 2: Variation in sea state parameters at positions spaced by 1h and 3h sailing distances at speeds 15, 20, and 25 knots on the route from Le Havre to Halifax. The statistics of the deviations are based on the formulas in Eqs (18)-(20).

	Diff(H_s) [m]		Diff(T_z) [s]		Diff(D_m) [deg]	
Δt	1h	3h	1h	3h	1h	3h
Speed = 15 knots:						
RMSE	0.15	0.41	0.21	0.57	15	26
RMSE*	4.8%	14%	3.3%	8.8%	N/A	N/A
Max	1.8	3.7	1.6	3.5	180	180
Max*	60%	170%	23%	51%	N/A	N/A
p95	0.32	0.89	0.44	1.2	17	50
p95*	9.7%	28%	7.0%	19%	N/A	N/A
Speed = 20 knots:						
RMSE	0.17	0.47	0.24	0.64	17	29
RMSE*	5.6%	16%	3.8%	9.9%	N/A	N/A
Max	1.9	4.8	1.8	3.5	180	180
Max*	57%	157%	24%	63%	N/A	N/A
p95	0.36	1.0	0.51	1.3	20	60
p95*	11%	32%	8.0%	21%	N/A	N/A
Speed = 25 knots:						
RMSE	0.19	0.52	0.28	0.71	18	31
RMSE*	6.4%	18%	4.3%	11%	N/A	N/A
Max	2.2	4.3	2.1	3.9	180	180
Max*	57%	162%	27%	79%	N/A	N/A
p95	0.41	1.1	0.58	1.5	24	68
p95*	13%	37%	9.2%	23%	N/A	N/A

*Relative difference; applicable to H_s and T_z only.

fit, but it is seen that it is *not*; in particular in case of the difference in mean wave direction. On the other hand, the t location-scale distribution fits nicely in almost all cases. The t location-scale distribution is useful for modeling data distributions with heavier tails than the normal distribution and, as its name indicates, it can model skewed distributions [41]. The distribution is controlled by the probability density function

$$f_t(x|\hat{\mu},\hat{\sigma},\nu) = \frac{\Gamma\left(\frac{\nu+1}{2}\right)}{\hat{\sigma}\sqrt{\nu\pi}\Gamma\left(\frac{\nu}{2}\right)}\left[\frac{\nu+\left(\frac{x-\hat{\mu}}{\hat{\sigma}}\right)^2}{\nu}\right]^{-\left(\frac{\nu+1}{2}\right)} \tag{21}$$

where $\Gamma(\cdot)$ is the gamma function, $\hat{\mu}$ is the location parameter, $\hat{\sigma}$ is the scale parameter, and ν is the shape parameter. It is noted that, generally, the location and scale parameters are dimensional, while the shape parameter is dimensionless. The PDF approaches the normal distribution as ν approaches infinity, and smaller values of ν yield heavier tails. The mean and the variance of the t location-scale distribution are

$$\text{mean} = \hat{\mu} \tag{22}$$

$$\text{var} = \hat{\sigma}^2\frac{\nu}{\nu-2} \tag{23}$$

The variance is only defined for values of $\nu > 2$; otherwise the variance is undefined.

It is noteworthy that, although not shown, the t location-scale distribution is also a good fit - and a much better fit than the normal distribution - in the cases of all the other routes, all speeds (15, 20, 25 knots) and both update intervals ($\Delta t =$ 1h and 3h) included. The descriptive "fitting" parameters of the PDFs for all the cases are given in Table 3, noting that the parameters for significant wave height and zero-upcrossing period apply to the relative differences, cf. Eqs. (18) and (19), and, as consequence, are dimensionless. The general observations from Table 3 are: (1) The location parameter $\hat{\mu}$ is positive for the difference in significant wave height in all cases. This is a coincidence but it is a reflection of the prevailing wind and wave systems in the studied ocean areas. Based on the definition, Eq. (18), the tendency thus is to observe smaller significant wave height as a voyage progresses; (2) The shape parameter ν takes relatively small values in all cases, and the observation from Figures 8 and 9 thus holds; that is, the t location-scale distribution, being a good fit to the data, is quite different from the normal distribution, and the normal distribution is in itself a poor fit in most of the cases. (3) The values of the scale parameter $\hat{\sigma}$, being comparable to standard deviation in qualitative terms, confirm that the largest variation in sea state parameters is encountered on the route Le

Havre to Halifax.

3.4. General remarks

The preceding subsections have shown that the spatio-temporal variation in sea state parameters along shipping routes can be significant; emphasising that the ERA5 data at the fixed grid points is taken as the ground truth. Moreover, the results are based on simulated shipping routes, where the ship speed, somewhat unrealistically, has been kept constant throughout, with no account for severe wave conditions. As such, the ”observed simulated” variation may not necessarily reflect the reality, not to say that the real variation is smaller. Another fact which should be mentioned in relation to real shipping and navigation is the use of weather routing, the role of which is to make ships avoid the worst sea states [42] by making the route path

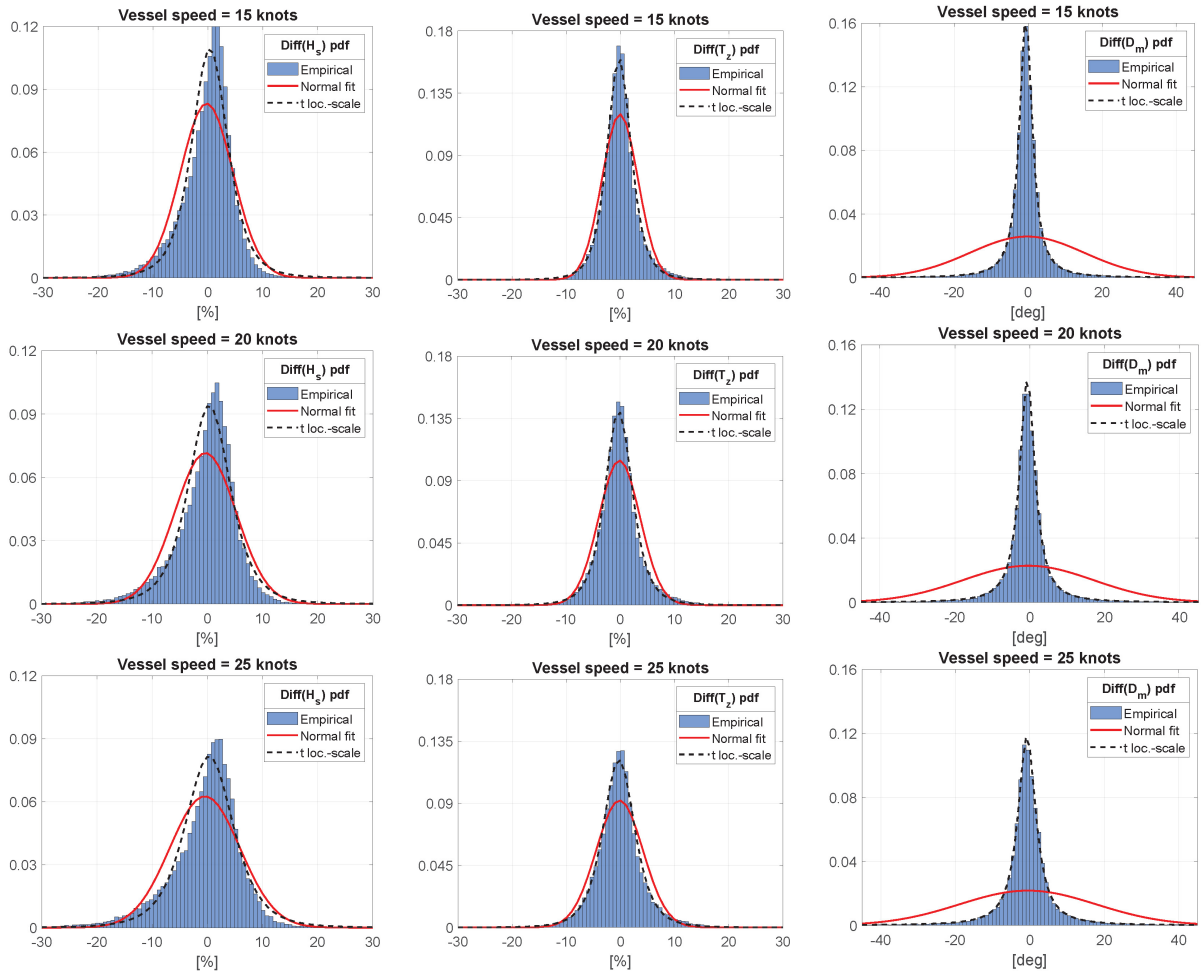

Figure 8: Probability density functions of the difference in sea state parameters, cf. Eqs. (18)-(20), when a sailing distance between consecutive waypoints equivalent to $\Delta t = 1$h is considered.

different as compared to the great circle path. Obviously, in reality, this could also influence the variation of sea state parameters encountered from ships.

From the last part of the study, considering the variation in sea state parameters encountered at consecutive waypoints spaced by the sailing distance in time Δt, it is evident that conditions can change a lot between 3-hour updates. In fact, the large variation in sea state parameters implies that the seaway, as encountered by a sailing ship during, say, 60 minutes up to 3h, in many cases is not the realisation of a stationary process, as normally assumed for ocean waves and the wave-induced load processes [43, 44]. Care should therefore be exercised in these cases if/when computing statistics of the wave-induced responses.

The study has been focused on variations in the sea state parameters, i.e. the integral wave parameters,

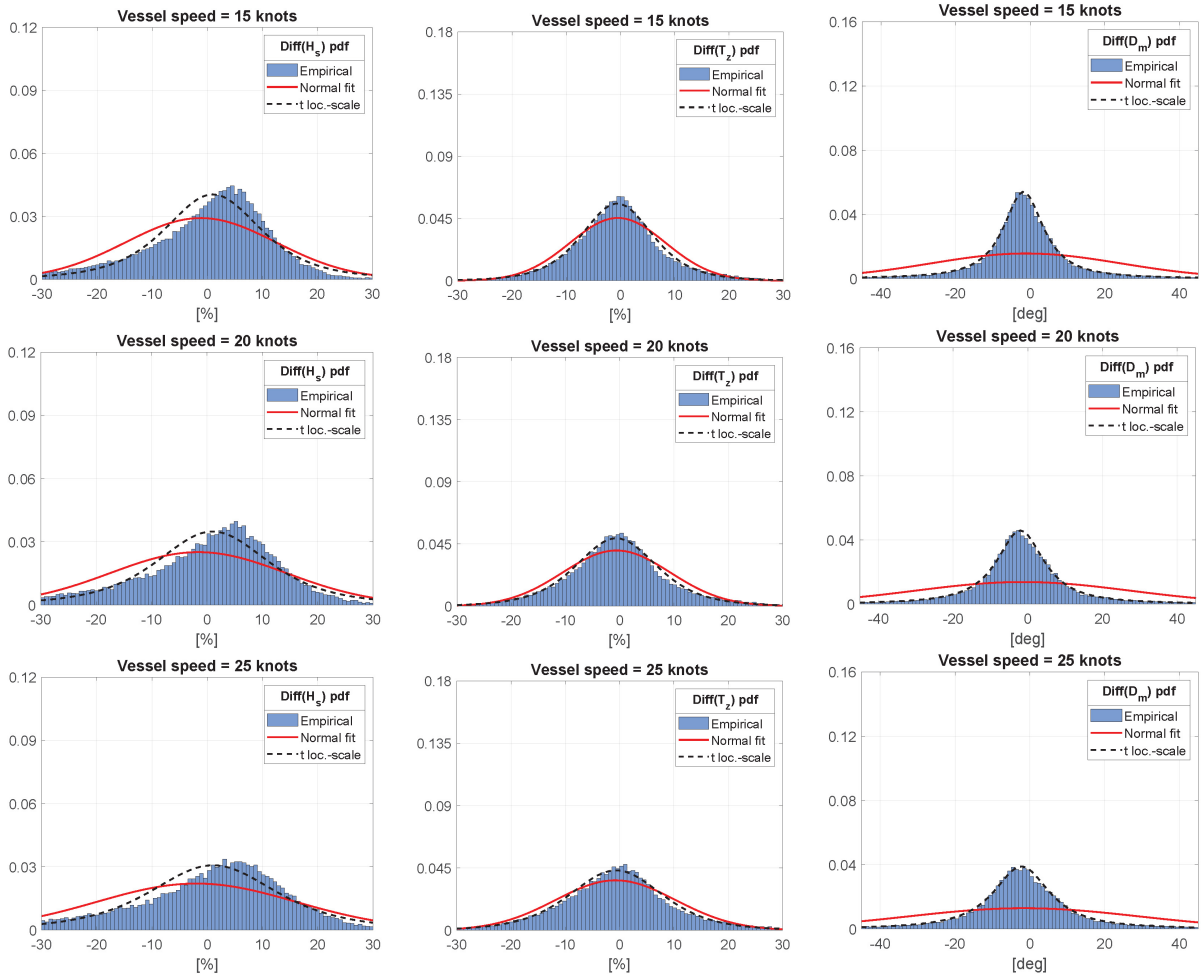

Figure 9: Probability density functions of the difference in sea state parameters, cf. Eqs. (18)-(20), when a sailing distance between consecutive waypoints equivalent to $\Delta t = 3$h is considered.

Table 3: Fit parameters used to establish the t-location scale PDF of the differences as calculated by Eqs. (18)-(20). Note that $\hat{\mu}$ is the location parameter (equivalent to mean value), $\hat{\sigma}$ is the scale parameters (equivalent to scaled standard deviation), and ν is the shape parameter.

	100·Diff(H_s) [-]			100·Diff(T_z) [-]			Diff(D_m) [deg]*		
Speed	$\hat{\mu}$	$\hat{\sigma}$	ν	$\hat{\mu}$	$\hat{\sigma}$	ν	$\hat{\mu}$	$\hat{\sigma}$	ν
Le Havre to Halifax									
$\Delta t = 1$h:									
15knots	.342	3.40	3.75	-.261	2.32	3.50	-.602	2.00	1.23
20knots	.348	3.97	3.76	-.284	2.65	3.46	-.671	2.37	1.23
25knots	.347	4.58	3.81	-.306	3.05	3.57	-.749	2.79	1.24
$\Delta t = 3$h:									
15knots	1.00	9.15	3.34	-.629	6.76	4.56	-1.80	6.17	1.31
20knots	1.02	10.6	3.38	-.654	7.70	4.71	-2.00	7.26	1.31
25knots	1.06	12.0	3.24	-.666	8.78	5.13	-2.23	8.61	1.35
Cadiz to Paramaribo									
$\Delta t = 1$h:									
15knots	.269	.995	1.68	.011	.905	1.95	-.374	.706	1.11
20knots	.297	1.09	1.55	.047	.989	1.91	-.491	.859	1.10
25knots	.332	1.22	1.56	.073	1.10	1.83	-.599	1.01	1.12
$\Delta t = 3$h:									
15knots	.741	2.86	1.85	.039	2.47	2.06	-1.11	2.13	1.20
20knots	.807	3.13	1.76	.132	2.70	2.05	-1.47	2.62	1.24
25knots	.929	3.51	1.82	.208	2.97	1.99	-1.79	3.07	1.27
Yokohama to Los Angeles									
$\Delta t = 1$h:									
15knots	.244	1.60	2.45	-.205	1.19	2.53	-.208	1.12	1.17
20knots	.164	2.09	2.81	-.186	1.38	2.35	-.160	1.46	1.22
25knots	.139	2.11	2.48	-.217	1.38	2.25	-.149	1.57	1.20
$\Delta t = 3$h:									
15knots	.593	4.54	2.76	-.546	3.39	2.89	-.626	3.38	1.22
20knots	.491	5.14	2.71	-.547	3.58	2.72	-.538	4.02	1.25
25knots	.263	6.01	2.87	-.602	3.96	2.72	-.461	4.78	1.31
Panama City to Auckland									
$\Delta t = 1$h:									
15knots	.120	1.34	1.96	.045	1.42	2.69	.426	1.14	1.18
20knots	.136	1.64	2.20	.039	1.66	2.96	.544	1.37	1.24
25knots	.133	1.83	2.11	.066	1.88	2.87	.634	1.60	1.23
$\Delta t = 3$h:									
15knots	.465	4.04	2.33	.182	4.12	3.27	1.36	3.50	1.24
20knots	.457	4.69	2.37	.159	4.58	2.97	1.64	4.11	1.24
25knots	.458	5.27	2.32	.248	5.20	2.97	1.92	4.81	1.24

*The shape parameter ν is dimensionless.

and hence the results only partly reflect the variation in the more detailed wave conditions in terms of

directional wave spectra. With the ultimate goal to consider the *consequence* of the spatio-temporal variation of wave conditions in relation to analyses of ship safety and fuel performance, it could be interesting to investigate the spatio-temporal variation in the details of the directional wave spectrum, when it is required in a position off the (ERA5) grid. In this case, however, it would be far from trivial how to make the interpolation, since wave dispersion, sea current, wind friction, etc. in principle have to be accounted for when the wave spectrum in a point off the fixed grid is wanted. Obviously, various approximations could lead the way, where the most simple one would be to simply interpolate in the single spectral components, frequency by frequency, using bilinear interpolation.

This study has focused solely on sea state parameters, emphasising that these include wave parameters only, while the implication and consequence in relation to practical applications in naval architecture and in ship performance evaluations, as mentioned, are left as work for the future. As such, the two points raised above, with respect to non-stationarity and the directional wave spectrum, introduce another concern related to spectral analysis and associated data processing, noting that relatively long time series sequences are necessary for, say, Fast Fourier Transformation to be reliable. For this type of future work, the dependency of the results on the discretisation could be investigated by repeating the analysis with datasets having a significantly lower or higher spatial and temporal resolution. Moreover, other metocean variables, notably wind, should be further included to have more clear and definitive conclusions on the consequence in regards to applications within naval architecture and ship performance monitoring.

4. Summary and main findings

Metocean data, notably integral wave parameters, or *sea state parameters*, are essential in studies related to evaluations of safety and fuel efficiency of marine designs and operations. Third generation spectral wave models formulated in terms of the energy balance equation and coupled with assimilation can provide this type of data, considering both temporal and spatial variations on a global scale. However, due to high computational efforts, results are computed in a discrete set of geographical points on a fixed grid, necessitating some sort of interpolation if positions off the grid are considered.

This paper has studied the variation in sea state parameters obtained from the ERA5 database [33], when special attention is given to mapped ship routes covered by ships sailing the typical service speed (15 – 20+ knots). Based on the study, the following findings are noteworthy in relation to applications within naval architecture and ship performance monitoring: (1) The level of spatial variation, for frozen

time, in the single sea state parameter, like significant wave height, zero-crossing period, and mean wave direction, can be substantial when the fixed grid points are considered; which in this study are spaced by 0.5 deg (longitude, latitude). (2) As a consequence of (1), it is *not* recommended to rely on interpolation using nearest neighbour but instead use bilinear interpolation, when sea state parameters are requested in a position off the grid considering a sailing ship. (3) The variation in sea state parameters at consecutive waypoints, spatio-temporally spaced by the sailing distance during the time Δt, can be large; especially, when $\Delta t = 3$h, but even for $\Delta t = 1$h, it will in many cases be questionable if the encountered seaway is the representation of a stationary process.

If the above findings are addressed in a perspective of practical applications concerned with, say, ship performance evaluations of efficiency and safety, finding (2) regarding interpolation scheme is trivial to introduce. On the other hand, findings (1) and (3) are nontrivial. In the strict sense, the finding (3) suggests that spectral analysis of wave-induced response recordings should be based on other means than Fast Fourier transformation that requires (sufficiently) long time windows to allow reliable estimation of the response spectra. In addition to the already mentioned (necessary) future work, e.g. subsections 3.2 and 3.4, future researches could therefore be dedicated to further development and analysis of spectral methods applicable in non-stationary conditions [45–50]. One particular application that would benefit by (improved) spectral methods for non-stationary data is the wave buoy analogy [10, 11] that facilitates realtime and on-site wave spectrum estimation using ship response measurements. Although the wave buoy analogy, generally, has been found to perform well, it would be interesting to investigate if improved estimation of sea state parameters was achieved in case of elaborate spectral calculations.

Acknowledgement

Sincere gratitude goes to one of the anonymous reviewers for a highly constructive and very comprehensive review leading to an improved manuscript. In addition, the author would like to thank Jesper Dietz (Maersk Line) and Philip Holt (MAN Energy Solutions) for sharing their views about the use of reanalyses and wave hindcasts. Finally, thanks go to Jørgen Juncher Jensen (DTU Mechanical Engineering) for useful comments about the manuscript. This work has been supported by the Research Council of Norway through the Centres of Excellence funding scheme, Project number 223254-AMOS.

References

[1] Copernicus Climate Change Service Information, ERA5: Fifth generation of ECMWF atmospheric reanalyses of the global

climate, copernicus Climate Change Service Climate Data Store (CDS): https://cds.climate.copernicus.eu/cdsapp#!/home accessed 08-02-2020 (2020).

[2] ECMWF, Part VII: ECMWF Wave Model, Tech. Rep. IFS Documentation Cy43r3, European Center For Medium-Range Weather Forecasts, Shinfield Park, Reading, RG2 9AX, England (2017).

[3] Hersbach et al., The ERA5 Global Reanalysis, Quarterly Journal of the Royal Meteorological Society (2020) DOI: 10.1002/qj.3803.

[4] O. Faltinsen, Sea Loads on Ships and Offshore Structures, Cambridge University Press, 1990.

[5] R. Beck, W. Cummins, J. Dalzell, P. Mandel, W. Webster, Vol. III: Motions in Waves and Controllability, in: E. Lewis (Ed.), Principles of Naval Architecture, Second Revision, SNAME, 1989, pp. 1–188.

[6] H. Tolman, B. Balasubramaniyan, L. Burroughs, D. Chalikov, Y. Chao, H. Chen, V. Gerald, Development and Implementation of Wind-Generated Ocean Surface Wave Models at NCEP, Weather and Forecasting 17 (2002) 311–333.

[7] The WAVEWATCH III Development Group, User manual and system documentation of WAVEWATCH III R version 6.07, https://github.com/NOAA-EMC/WW3/wiki/Manual (2019).

[8] F. Ardhuin, J. Stopa, B. Chapron, F. Collard, R. Husson, R. Jensen, J. Johannessen, A. Mouche, M. Passaro, D. Quartly, V. Swail, I. Young, Observing sea states, Ocean Frontiers 6 (2019) Article 124.

[9] S. Barstow, J.-R. Bidlot, S. Caires, M. Donelan, W. Drennan, H. Dupuis, H. Graber, J. Green, O. Gronlie, C. Gurin, Measuring and Analysing the Directional Spectrum of Ocean Waves, COST Office, 2005.

[10] U. D. Nielsen, A concise account of techniques available for shipboard sea state estimation, Ocean Engineering 129 (2017) 352–362.

[11] U. D. Nielsen, J. Dietz, Estimation of sea state parameters by the wave buoy analogy with comparisons to third generation spectral wave models, Ocean Engineering 216 (2020) 107781.

[12] P. Janssen, The Interaction of Ocean Waves and Wind, Vol. Online version, ISBN 9780511525018, Cambridge University Press, 2009.

[13] F. Ardhuin, A. Orfila, Wind waves, in: E. Chassignet, A. Pascual, J. Tintore, J. Verron (Eds.), New Frontiers in Operational Oceanography, GODAE OceanView, 2018, pp. 393–422.

[14] F. Ardhuin, Ocean waves in geosciences, Laboratoire d'Oceanographie Physique et Spatiale, Brest, France, 2020.

[15] N. Schade, H. Heinrich, G. Rosenhagen, Regional evaluation of ERA-40 reanalysis data with marine atmospheric observations in the North Sea Area, Meteorologische Zeitschrift 22 (2013) 675–684.

[16] R. Campos, C. Guedes Soares, Comparison and assessment of three wave hindcasts in the North Atlantic Ocean, Journal of Operational Oceanography 9 (2016) 26–44.

[17] B. Kvamme, A. Orimolade, S. Haver, O. Gudmestad, Marine Operation Windows Ofsshore Norway, in: Proc. 35th Int'l Conference on Ocean, Offshore and Arctic Engineering, Busan, South Korea, 2016.

[18] Copernicus Climate Change Service (C3S), Ship performance along standard shipping routes derived from reanalysis and seasonal forecasts, https://cds.climate.copernicus.eu/cdsapp#!/dataset/sis-shipping-consumption-on-routes?tab=doc (2018).

[19] A. Magnusson, O. Vårdal, B. Hjollo, R. MyMebust, M. Reistad, K. Hansen, Forecasting Wave-Induced Response For Offshore Floating Structures, in: Proc. of 11th ISOPE, Stavanger, Norway, 2001.

[20] R. G. Standing, Review of the role of response forecasting in decision-making for weather-sensitive offshore operations,

BMT Fluid Mechanics Limited for the Health and Safety Executive Report 347, BMT (2005).

[21] L. Perera, B. Mo, An overview of data veracity issues in ship performance and navigation monitoring, in: Proc. of 37th OMAE, no. OMAE2018-77669, ASME, Madrid, Spain, 2018.

[22] T. Dickson, H. Farr, D. Sear, J. Blake, Uncertainties in data for the offshore environment, Applied Ocean Research 88 (2019) 138–146.

[23] L. De Gracia, H. Wang, W. Mao, N. Osawa, I. Rychlik, G. Storhaug, Comparison of two statistical wave models for fatigue and fracture analysis of ship structures, Ocean Engineering 187 (2019) 106161.

[24] I. Thompson, Virtual hull monitoring of a naval vessel using hindcast data and reconstructed 2-D wave spectra, Marine Structures 71 (2020) 102730.

[25] B. Taskar, P. Andersen, Benefit of speed reduction for ships in different weather conditions, Transportation Research Part D: Transport and Environment 85 (2020) DOI: 10.1016/j.trd.2020.102337.

[26] M. Schirmann, M. Collette, J. Gose, Impact of weather source selection on time-and-place specific vessel response predictions, in: Trends in the Analysis and Design of Marine Structures - Proc. 7th International Conference on Marine Structures, Dubrovnik, Croatia, 2019.

[27] E. Bitner-Gregersen, A. Magnusson, Effect of intrinsic and sampling variability on wave parameters and wave statistics, Ocean Dynamics 64 (2014) 1643–1655.

[28] S. Uppala et al., The ERA-40 reanalysis, Quarterly Journal of the Royal Meteorological Society 131 (2005) 2961–3012.

[29] D. Dee et al., The ERA-Interim reanalysis: configuration and performance of the data assimilation system, Quarterly Journal of the Royal Meteorological Society 137 (2011) 553–597.

[30] G. Komen, L. Cavaler, M. Donelan, K. Hasselmann, S. Hasselmann, P. Janssen, Dynamics and Modelling of Ocean Waves, Cambridge University Press, 1994.

[31] The WISE Group, L. Cavaleri et al., Wave modelling - The state of the art, Progress in Oceanography 75 (2007) 603–674.

[32] F. Ardhuin, E. Rogers, A. Babanin, J. Filipot, R. Magne, A. Roland, A. van der Westhuysen, P. Queffeulou, J. Lefevre, L. Aouf, F. Collard, Semiempirical dissipation source functions for ocean waves. Part I: Definition, calibration, and validation, Journal of Physical Oceanography 40 (2010) 1917–1941.

[33] Hersbach et al., ERA5 hourly data on single levels from 1979 to present, https://cds.climate.copernicus.eu/cdsapp#!/dataset/reanalysis-era5-single-levels?tab=overview (Accessed: 30-01-2020), DOI: 10.24381/cds.adbb2d47.

[34] R. Bannister, Elementary 4D-VAR, Tech. Rep. DARC Technical Report No. 2, Data Assimilation Research Centre, University of Reading, UK (2007).

[35] M. Toews, Ncep t62 gaussian grid, https://commons.wikimedia.org/wiki/File:NCEP_T62_gaussian_grid.png, accessed: 30-01-2020.

[36] ERA5: What is the spatial reference, https://confluence.ecmwf.int/display/CKB/ERA5%3A+What+is+the+spatial+reference, accessed: 30-01-2020.

[37] M. K. Ochi, Ocean Waves - The Stochastic Approach, Cambridge University Press, 1998.

[38] DNV-GL, Recommended Practice DNV-RP-C205: Environmental conditions and environmental loads, Høvik, Norway, 2014.

[39] C. Fernandez, M. Steel, On Bayesian modeling of fat tails and skewness, J. American Statistical Assoc. 93 (1998) 359–371.

[40] F. Leisen, L. Rossini, C. Villa, Loss-based approach to two-piece location-scale distributions with applications to dependent data, Statistical Methods and Applications 29 (2019) 309–333.

[41] MATLAB R2020b, t Location-Scale Distribution, `https://se.mathworks.com/help/stats/t-location-scale-distribution.html` (Accessed: 28-12-2020).

[42] A. Olsen, C. Schrøter, J. Jensen, Wave height distribution observed by ships in the North Atlantic, Ships and Offshore Structures 1 (2005) 1–12.

[43] O. F. Hughes, Ship Structural Design, SNAME, USA, 1988.

[44] J. J. Jensen, Load and Global Response of Ships, Vol. 4 of Elsevier Ocean Engineering Book Series, Elsevier, 2001.

[45] T. Iseki, D. Terada, Study on Real-time Estimation of the Ship Motion Cross Spectra, Journal of Marine Science and Technology 7 (2003) 157–163.

[46] T. Iseki, Real-time Analysis of Higher Order Ship Motion Spectrum, in: Proc. of OMAE 2010, ASME, Shanghai, China, 2010.

[47] T. Iseki, Non-stationary Ship Motion Analysis Using Discrete Wavelet Transform, in: Proc. 8th Int'l Conference on the Stability of Ships and Ocean Vehicles (STAB), Glasgow, Scotland, 2012.

[48] K. Ohtsu, H. Peng, G. Kitagawa, Time Series Modeling for Analysis and Control: Advanced Autopilot and Monitoring Systems, JSS Research Series in Statistics, Springer, 2015.

[49] T. Takami, U. D. Nielsen, J. J. Jensen, Wave-induced Response Prediction Using Prolate Spheroidal Wave Function, in: Proc. 20th Nordic Maritime Universities Workshop, Hamburg, Germany, 2020.

[50] T. Takami, U. D. Nielsen, J. J. Jensen, Estimation of Autocorrelation Function and Spectrum Density of Wave-induced Responses Using Prolate Spheroidal Wave Functions, Journal of Marine Science and Technology (Accepted for publication) DOI: https://doi.org/10.1007/s00773-020-00768-9.